JOURNAL OF THE KOREAN ASTRONOMICAL SOCIETY
38: 175 ~ 178, 2005

DARK ENERGY REFLECTIONS IN THE REDSHIFT-SPACE QUADRUPOLE

HIROAKI NISHIOKA[1], KAZUHIRO YAMAMOTO[2], AND BRUCE A. BASSETT[3,4]
[1] Institute of Astronomy and Astrophysics, Academia Sinica, Taipei 106, Taiwan, R.O.C.
E-mail: nishioka@asiaa.sinica.edu.tw
[2] Department of Physical Science, Hiroshima University, Higashi-Hiroshima, 739-8526, Japan
E-mail: kazuhiro@hiroshima-u.ac.jp
[3] Department of Physics, Kyoto University, Kyoto,739-8502, Japan
[4] Institute of Cosmology and Gravitation, University of Portsmouth, Portsmouth PO1 2EG, UK
E-mail: Bruce.Bassett@port.ac.uk
(Received February 1, 2005; Accepted March 15, 2005)

ABSTRACT

We show that next-generation galaxy surveys such as KAOS (the Kilo-Aperture Optical Spectrograph)will constrain dark energy even if the baryon oscillations are missing from the monopole power spectrum and the bias is scale- and time-dependent. KAOS will accurately measure the quadrupole power spectrum which gives the leading anisotropies in the power spectrum in redshift space due to peculiar velocities, the finger of God effect, as well as the Alcock-Paczynski effect. The combination of monopole and quadrupole power spectra powerfully breaks the degeneracy between the bias parameters and dark energy and, in the complete absence of baryon oscillations ($\Omega_b = 0$), leads to a roughly 500% improvement in constraints on dark energy compared with the monopole spectrum alone. As a result, for KAOS the worst case with no oscillations has dark energy errors only mildly degraded relative to the ideal case, providing insurance on the robustness of KAOS constraints on dark energy. We show that nonlinear effects are crucial in correctly evaluating the quadrupole and significantly improving the constraints on dark energy when we allow for multi-parameter scale-dependent bias.

Key words : cosmological parameters — cosmology: theory — galaxies: distances and redshifts — large-scale structure of universe — methods: analytical

I. INTRODUCTION

The promise of next-generation galaxy surveys such as KAOS (the Kilo-Aperture Optical Spectrograph) is to map the distribution of about one million galaxies in the redshift range $z = 0.5 - 3.5$. This redshift coverage will allow the baryon oscillations in the matter power spectrum to be followed as they were stretched by the cosmic expansion, thus providing us with a standard ruler with which to precisely measure the extragalactic distance scale and expansion rate. (Eisenstein 2004, Blake & Glazebrook 2003, Linder 2003, Seo & Eisenstein 2003, Hu & Haiman 2003, Amendola, Quercellini & Giallongo, 2004)

However, this technique relies crucially on the assumption that the baryon oscillations will be detected. Although there are tentative indications for this at low-z in the 2df data (Miller, Nichol & Chen 2002, Yamamoto 2004) the jury is still out on their existence. If bias turns out to be much more complicated than we think or Ω_b is unexpectedly low we may face an essentially featureless galaxy power spectrum that is too slippery to extract a standard ruler from. In that case it is natural to ask whether surveys such as KAOS will yield any constraints on dark energy.

The aim of this paper is to show that *even* in this worst case scenario, next-generation surveys will be able to deliver good constraints on dark energy through a very different route: redshift-space anisotropies and the Alcock-Paczynski (AP) effect (Alcock & Paczynski 1979, Ballinger, Peacock & Heavens 1996, Yamamoto 2003, Yamamoto 2004).

In general the power spectrum in redshift space is not isotropic; an effect already seen in the 2df survey (Peacock, *et al.* 2001). There is a linear distortion due to the bulk motion of the sources within the linear theory of density perturbation (Kaiser 1987), while the finger of God effect causes radial elongations due to the motion of galaxies in the nonlinear regime (Peacock & Dodds 1994). In addition there is a geometric distortion due to the AP effect related to the distance-redshift relation of the universe. As a result the redshift-space power spectrum depends on the angle θ between the line-of-sight direction γ and the wave number vector $\mathbf{k}$ (see e.g., Suto *et al.* 1999).

In general the redshift-space power spectrum can be expanded as (Taylor & Hamilton 1996):

$$P(\mathbf{k}, z) = P(k, \mu, z) = \sum_{l=0,2,4\cdots} P_l(k, z)\mathcal{L}_l(\mu), \qquad (1)$$

where $\mathcal{L}_l(\mu)$ is the Legendre polynomial, $\mu = \cos\theta$ and

Proceedings of *the 6th East Asian Meeting of Astronomy*, held at Seoul National University, Korea, from October 18-22, 2004.

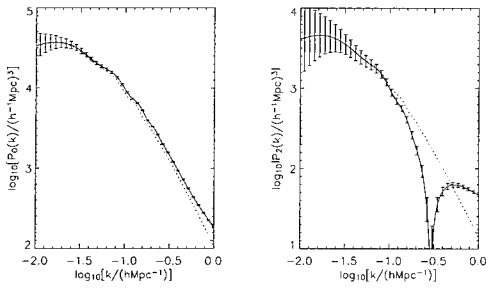

Fig. 1.— KAOS1 constraints on the multipole moments of the power spectrum, $\langle \mathcal{P}_0(k) \rangle$ and $\langle \mathcal{P}_2(k) \rangle$ for linear (dotted lines) and nonlinear (solid lines) spectra respectively. The sign of the nonlinear $< \mathcal{P}_2(k) >$ prediction changes from positive to negative as k becomes large. The KAOS1 ($z < 1.5$) sample is assumed and we fixed $n = 1$, $h = 0.7$, $\Omega_b = 0.045$, $\Omega_m = 0.28$ and $w = -1$. For the bias we adopted $b_0 = 1.35$, $p_0 = 1$ for the linear model, $p_1 = 1$, $b_1 = 0.1$, $\nu = 1$ for the nonlinear spectrum. The higher moments $P_\ell, \ell \geq 4$ are not well-constrained even by KAOS.

$k = |\mathbf{k}|$. The odd moments vanish by symmetry.

The monopole $P_0(k, z)$ represents the angular averaged power spectrum and has been investigated in great depth in the 2df and SDSS surveys. $P_2(k, z)$ is the quadrupole spectrum and gives the leading anisotropic contribution. As can be seen in Fig. 1 it will be well-constrained even by just the $z < 1.5$ sample, which we label KAOS1 (see Table 1 for definitions). The higher order multipoles are not well-constrained however.

Crucially, the multipole moments reflect different aspects of the redshift distortions in the power spectrum which can therefore aid in breaking degeneracies between the cosmological parameters, bias and dark energy. The purpose of this paper is to consider the extent to which the anisotropic component of the power spectrum, P_ℓ, $\ell \geq 2$, gives new information about dark energy via the nonlinear effects and the geometric (AP) distortion.

II. FORMALISM

Here we employ the Fisher matrix approach in order to estimate the accuracy to which we can constrain the equation of state of the dark energy with a measurement of the power spectrum. In general the Fisher matrix is defined by $F_{ij} = -\langle \partial^2 \ln L / \partial\theta_i \partial\theta_j \rangle$, where L is the likelihood of a data set given the model parameters θ_i. Assuming a Gaussian probability distribution function for the errors of a measurement of the multipole power spectrum $\mathcal{P}_l(k)$, the Fisher matrix for each multipole spectrum is

$$F_{ij}^{(l)} \simeq \frac{1}{4\pi} \int_{k_{\rm min}}^{k_{\rm max}} \kappa_l(k) \frac{\partial \langle \mathcal{P}_l(k) \rangle}{\partial \theta_i} \frac{\partial \langle \mathcal{P}_l(k) \rangle}{\partial \theta_j} k^3 d\ln k, \quad (2)$$

where $\kappa_l(k)$ is the effective volume of the survey available for measuring the ℓ-th power spectrum at wavenumber k:

$$\kappa_l(k)^{-1} = \frac{1}{2} \int_{-1}^{1} d\mu \int d\mathbf{s} \bar{n}(\mathbf{s})^4 \times \psi(\mathbf{s}, k, \mu)^4 \left[P(k, \mu, z) + 1/\bar{n}(\mathbf{s}) \right]^2 [\mathcal{L}_l(\mu)]^2 \times \left[\int d\mathbf{s}' \bar{n}(\mathbf{s}')^2 \psi(\mathbf{s}', k, \mu)^2 \right]^{-2}, \quad (3)$$

and

$$\langle \mathcal{P}_l(k) \rangle = \frac{1}{2} \int_{-1}^{1} d\mu \frac{\int d\mathbf{s} \bar{n}(\mathbf{s})^2 \psi(\mathbf{s}, k, \mu)^2 P(k, \mu, z) \mathcal{L}_l(\mu)}{\int d\mathbf{s}' \bar{n}^2(\mathbf{s}') \psi(\mathbf{s}', k, \mu)^2} \quad (4)$$

where $\psi(\mathbf{s}, k, \mu)$ is a weight factor that we can choose freely, $\bar{n}(\mathbf{s})$ is the mean number density, and $\mathbf{s}$ denotes the three dimensional coordinate in redshift space. This formula can be derived in a similar way to obtain the optimal weighting scheme (see e.g., Feldman Kaiser & Peacok 1994, Yamamoto 2003).

Minimizing the variance on the power spectrum gives $\psi(\mathbf{s}, k, \mu) = [1 + \bar{n}(\mathbf{s}) P(k, \mu, z)]^{-1}$, the same as used by Seo & Eisenstein (2003).

Next we explain our theoretical modelling of the power spectrum. In a redshift survey, the redshift z is the indicator of the distance. Therefore we need to assume a distance-redshift relation $s = |\mathbf{s}| = s[z]$ to plot a map of objects. The power spectrum depends on this choice of the radial coordinate of the map $s = s[z]$ due to the geometric distortion (AP) effect. For our fiducial background we adopt a flat universe with $\Omega_m = 0.3$. Here $H_0 = 100\ h$km/s/Mpc is the Hubble parameter.

We consider a cosmological model with the dark energy component with constant equation of state, $w \equiv p/\rho$, since estimates for the nonlinear power spectrum in more general cases do not yet exist. Then, we have

$$r(z, \Omega_m, w) = \frac{1}{H_0} \int_0^z \frac{dz'}{\sqrt{\Omega_m (1+z')^3 + (1-\Omega_m)(1+z')^{-3(1+w)}}}, \quad (5)$$

Our fiducial model thus has $s(z) \equiv r(z, 0.3, -1)$. The geometric distortion in the power spectrum depends on $r(z, \Omega_m, w)$ and the power spectrum at redshift z is described by scaling the wave numbers from real space to redshift space via $q_\parallel \to k\mu/c_\parallel$ and $q_\perp \to k\sqrt{1-\mu^2}/c_\perp$ with $c_\parallel(z) = dr(z)/ds(z)$ and $c_\perp(z) = r(z)/s(z)$.

We write the galaxy power spectrum in nonlinear theory as

$$P_{\rm gal}(q_\parallel, q_\perp, z) = \left(1 + \frac{f(z)}{b(z,q)} \frac{q_\parallel^2}{q^2} \right)^2 b(z,k)^2 P_{\rm mass}^{\rm NL}(q, z) D[q_\parallel], \quad (6)$$

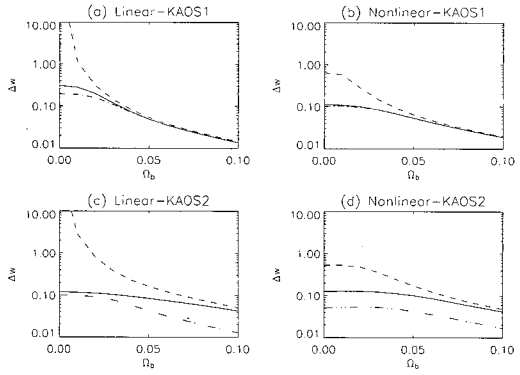

Fig. 2.— Error estimates on w as a function of Ω_b. The left panels (a) and (c) are the results using the linear spectrum and the right panels (b) and (d) are the nonlinear spectrum. The dashed curve is the result utilizing *only* $\mathcal{P}_0(k)$, the dotted curve is the result with *only* $\mathcal{P}_2(k)$, the solid curve is the result obtained using *both* $\mathcal{P}_0(k)$ and $\mathcal{P}_2(k)$. The target parameters here are same as those in Fig. 1. The low-redshift sample, KAOS1, is assumed in (a) and (b), the high-redshift sample, KAOS2, is assumed in (c) and (d). The dotted-dashed curve in (a) and (b) shows the constraint combining all $\mathcal{P}_0(k)$ to $\mathcal{P}_6(k)$. The double dotted-dashed curve in (c) and (d) shows the constraint obtained from the full KAOS sample (KAOS1 + KAOS2). The key point is how flat the resulting curve is for $\Omega_b \leq 0.05$ despite the absence of baryon oscillations for $\Omega_b \to 0$.

with $f(z) = d\ln D_1(z)/d\ln a(z)$, where $q^2 = q_\parallel^2 + q_\perp^2$, $b(z,q)$ is a scale-dependent bias factor, $P_{\rm mass}^{\rm NL}(q,z)$ is the nonlinear mass power spectrum normalized by $\sigma_8 = 0.9$, $D_1(z)$ is the linear growth rate, and $a(z)$ is the scale factor. The term in proportion to $f(z)$ describes the linear distortion (Kaiser 1987). $D[q_\parallel]$ represents the damping factor due to the finger of God effect. Assuming an exponential distribution function for the pair wise peculiar velocity (Mo, Jing & Boerner 1997, Magira, Jing & Suto 1997, Suto, Magira & Yamamoto 2000) gives $D[q_\parallel] = 1/(1+(q_\parallel\sigma_P)^2/2)$, where σ_P is the 1-dimensional pair wise peculiar velocity dispersion estimated by Mo, Jing & Boerner (1997).

For $P_{\rm mass}^{\rm NL}(q,z)$ we adopt the fitting formula for the quintessence cosmological model (Ma *et al.* 1999).

We then use the fitting formula for $f(z)$ developed by Wang & Steinhardt (1998). For the nonlinear modelling, we assume a scale dependent bias model where the correction depends on the wave number in proportion to $1 + AD_1(z)^\zeta q^\nu$, where A, ζ and ν are bias constants. For convenience, we write

$$b(z,k) = \left(1 + \frac{b_0 - 1}{D_1(z)}\right)\left[1 + b_1\left(\frac{D_1(z)^{p_1} q}{0.1\ h{\rm Mpc}^{-1}}\right)^\nu\right], \quad (7)$$

where b_0, b_1, p_1 and ν are the nonlinear bias constants. In the linear case the bias is scale-*independent* and given by $b(z) = 1 + (b_0 - 1)D_1(z)^{-p_0}$ where p_0 is a constant.

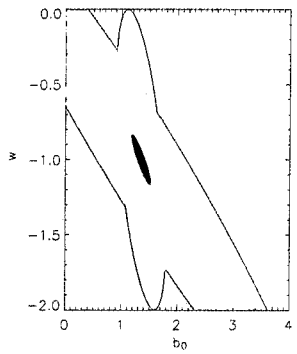

Fig. 3.— 2-d likelihood for $\mathcal{P}_0$ alone (vertical ellipse), $\mathcal{P}_2$ alone (large light blue ellipse) and the combination (small dark blue ellipse). The large improvement comes from the simultaneous improvement in all the other parameters marginalized over, showing the potential of combining monopole and quadrupole power spectra. Here the same parameters are used excepting $\Omega_b = 0$.

III. RESULTS

Fig. 1. shows the monopole and quadrupole power spectra $\langle\mathcal{P}_0(k)\rangle$ and $\langle\mathcal{P}_2(k)\rangle$ for the linear and nonlinear models described above, assuming the KAOS1 sample described in Table 1. $\langle\mathcal{P}_0(k)\rangle$ is positive while the nonlinear effects cause $\langle\mathcal{P}_2(k)\rangle$ to change sign at large k. For $\langle\mathcal{P}_0(k)\rangle$, the linear power spectrum agrees well with the nonlinear power spectrum because the two nonlinear contributions to it cancel out: the finger of God effect decreases the amplitude while $P_{\rm mass}(k)$ increases the amplitude due to the nonlinearity at large k. By comparison, it is very clear that the linear theory is not good for the higher multipole moments on small scales, $k \gtrsim 0.1h{\rm Mpc}^{-1}$.

TABLE 1.

	KAOS1	KAOS2
redshift range	$0.5 < z < 1.5$	$2.5 < z < 3.5$
survey area (deg^2)	10^3	150
$\bar{n}$ (h^{3}Mpc^{-3})	10^{-4}	10^{-4}
$k_{\rm max}$ (hMpc^{-1})	0.4	1
b_0	1.35	1.75

The parameters of the samples used in our analysis. $\bar{n}$ is the average number density, $k_{\rm max}$ is the maximum wavenumber in evaluating the Fisher matrix elements.

Now let us investigate the details of the Fisher matrix elements. We assume the KAOS1 and KAOS2 samples, whose details are summarized in Table 1. The precision with which w can be recovered is shown in Fig 2. To produce these estimates we have marginalized over Ω_m and all the bias parameters, i.e. we quote $\Delta w \equiv (\mathbf{F}^{-1/2})_{ww}$. In the linear case we marginalize over b_0 and p_0 while in the nonlinear case we marginalize over b_0, p_1, b_1 and ν. Since the bias may be constrained by other methods (lensing or higher-order

correlation function) our results are conservative.

Fig. 2. shows Δw as a function of Ω_b. The left panels are the results for the linear perturbation theory, while the right panels are the nonlinear model. The upper panels assume the KAOS1 sample, while the lower panels assume the KAOS2 sample. In general, Δw becomes larger as the baryon fraction becomes smaller since the baryon oscillations become less and less distinct. As Ω_b becomes smaller, the contribution from $\mathcal{P}_2$ becomes increasingly important. It is clear from the dashed curve that the constraint on w from $\mathcal{P}_0$ is very weak around $\Omega_b = 0$ because the baryon oscillations disappear, taking with it the standard ruler. This is the same for the dotted curve which shows the constraints from $\mathcal{P}_2$.

One of the main results of this paper is the solid curve which shows the constraint from the combination of $\mathcal{P}_0$ and $\mathcal{P}_2$. It is good even in the case $\Omega_b = 0$ when the baryon oscillation are missing from the matter power spectrum, implying that the geometric distortion (AP test) plays the central role in constraining w. This does not depend on the bias parameters. Inclusion of a constant parameter for the stochastic bias does not alter our results (Tegmark & Peables 1998).

It is interesting to consider the reason why the constraint on Δw from the combination of $\mathcal{P}_0$ and $\mathcal{P}_2$ is so much better than from either one considered separately. To evaluate Δw, we marginalized over the bias parameters and Ω_m. The combination of $\mathcal{P}_0$ and $\mathcal{P}_2$ improves the constraint on w by breaking degeneracies in the bias-dark energy parameter space, as can be clearly seen in Fig. 3 which shows the resulting 2-d likelihood ellipses.

$\mathcal{P}_2$ particularly breaks the degeneracies between w and Ω_m and the bias parameters in the nonlinear case. In particular the combination of $\mathcal{P}_0$ and $\mathcal{P}_2$ provides independent information about the bias, extending the well-recognized fact that $\mathcal{P}_2$ gives information about the bias (e.g. Taylor & Hamilton 1996).

IV. CONCLUSIONS

We have investigated the accuracy with which we can expect next-generation galaxy surveys such as KAOS to measure the multipole moments of the anisotropic power spectrum in redshift space and the resulting improvements in dark energy constraints.

We found a number of key results: (1) the quadrupole is very useful in breaking degeneracies between bias and dark energy. (2) Nonlinear effects have a substantial influence on the quadrupole and higher multipoles at the scale $k \gtrsim 0.1h\mathrm{Mpc}^{-1}$. The inclusion of the nonlinear power spectrum enhances the precision with which the dark energy can be constrained because the nonlinear effects increase the power at small scale which is also where constraints are good. (3) Applying these results to dark energy in a specific case based on the KAOS survey we have found that significant constraints arise even if there are no baryon oscillations in the monopole spectrum and allowing for multi-parameter scale-dependent bias by combining the monopole and quadrupole spectra. Inclusion of a constant parameter for stochastic bias does not alter our conclusion.

This is a key piece of insurance for large galaxy surveys given current uncertainty about the existence of baryon oscillations and ensures that large, next-generation, galaxy surveys will make a significant contribution to the hunt for dark energy irrespective of the existence of baryon oscillations.

ACKNOWLEDGEMENTS

This paper is based on Yamamoto, Bassett and Nishioka (2005).

REFERENCES

Alcock, C., & Paczynski, B., 1979, Nature, 281, 358

Amendola, L., Quercellini, C., & Giallongo, E., 2004, arXiv:astro-ph/0404599

Ballinger, W. E., Peacock, J.A., & Heavens, A. F., 1996, MNRAS, 282, 877

Blake, C., & Glazebrook, K., 2003 ,ApJ, 594, 665

Eisenstein, D., 2003, Proc. WFMOS conference, arXiv:astro-ph/0301623.

Feldman, H. A., Kaiser, N. & Peacock, J. A., 1994, ApJ, 426, 23

Hu, W., & Haiman, Z., 2003, PRD, 68, 063004

Kaiser, N., 1987 MNRAS, 227, 1

KAOS, http://www.noao.edu/kaos/

Linder, E. V., PRD, 2003, 68, 083504

Ma, C-P., Caldwell, R. R., Bode, P., & Wang L., 1999, ApJL, 521, L1

Magira, H., Jing, Y. P., & Suto, Y., 1997, ApJ, 528, 30

Matsubara, T., & Suto, Y., 1996, ApJ, 470, L1

Matsubara, T. & Szalay, A. S., 2003, PRL., 90, 1302

Miller, C. J., Nichol, R. C., & Chen, X. I., 2002, ApJ, 579, 483

Mo, H-J., Jing, Y. P., & Boerner, G., 1997, MNRAS, 286, 979

Peacock, J. A. *et al.* ., 2001, Nature, 410, 169

Peacock, J. A. & Dodds, S. J., 1994, MNRAS, 267, 1020

Seo, H-J, & Eisenstein, D. J., 2003, ApJ, 598, 720

Suto, Y., Magira, H., Jing, Y. P., Matsubara, T., & Yamamoto, K., 1999, PTPS. 133, 183

Suto, Y., Magira, H., & Yamamoto, K., 2000, PASJ, 52, 249

Taylor, A. N., & Hamilton A. J. S., 1996,MNRAS, 282, 767

Tegmark, M., & Peebles, P. J. E., 1998, ApJ, 500, L79

Wang, L., & Steinhardt, P. J., 1998, ApJ, 508, 483

Yamamoto, K., 2003, ApJ, 595, 577

Yamamoto, K., 2004,ApJ, 605, 620

Yamamoto, K., Bassett, B. A., & Nishioka, H., 2005,PRL, in press, arXiv:astro-ph/0409207